Graduate Student Summer Program 2010

Satellite Observation of Biomass Burning Emissions

BIEBELE ABEL

MORGAN STATE UNIVERSITY

DEPARTMENT OF CHEMISTRY

(SUMMER PROGRAM IN CLIMATE AND RADIATION BRANCH, NASA/GSFC)

MENTOR: Dr CHARLES ICHOKU

NASA Goddard Space Flight Center

Abstract

Human activity has increased the concentration of the earth's atmospheric carbon dioxide (CO_2) and carbon monoxide (CO), which play a direct role in contributing to global warming (Boering et al., 1996). Wildfires and other types of biomass-burning affect vast area of forest lands, grass lands, and agricultural lands across the globe annually, and consume an estimated 5500 — 9200 Tg of biomass. Such fires often release intense heat energy, which is propagated by conduction, convection, and radiation. Fire radiative energy (FRE), like other types of electromagnetic radiant energy, propagates in space and can be remotely sensed with appropriate instruments from satellite. In this research study, 4 different regions were selected: West Africa, Brazil (Amazon), Congo Basin and Alaska. The satellite measurements of Aerosol, CO and CO_2 were extracted, and compared with the satellite measurements of Fire radiative energy (FRE) release rates or Power (FRP) to examine the interrelationships between them in each region.

INTRODUCTION

Human evolution and the use of fire have gone hand in hand ever since the origin of our species in the savannas and woodlands of Africa (Schüle, 1990). Biomass burning affects most vegetated landscapes around the world to various degrees and intensities. Some biomass fires originate by accident or as a result of such natural causes such as lighting, while others are deliberately ignited for agricultural or experimental purposes. Open biomass fires emit massive amount of smoke, which can be transported over distances ranging from a few to thousands of kilometers. The smoke is composed of aerosol and a large variety of trace gases (CO, CO_2, CH_4, non methane hydrocarbons, and other compounds).

Carbon monoxide (CO) is a trace atmospheric constituent that plays an important role in troposphere chemistry as a major sink for hydroxide (OH) (Logan et al., 1981). Atmospheric CO_2 concentration has risen since pre-industrial times from ~ 280 ppm to ~ 380 ppm today (Indermühle et al., 1999; Conway et al., 1994). The principal reason for this trend is increase in emissions associated with human activities, such as combustion of fossil fuel, (Keeling et al., 1989). Carbon dioxide is one of the most important and long-lived anthropogenic greenhouse gases (Intergovernmental Panel on Climate Change, 2001).

Measurements of Fire Radiative Energy (FRE) are currently being provided with specialized space-borne sensors, such as the Moderate Resolution Imaging Spectro-radiometer (MODIS) aboard the Earth Observing System (EOS) Terra and Aqua polar orbiting satellites (Kaufman et al., 1998). The Aqua satellite, which was launched by NASA in May 2002, also carries the Atmospheric Infrared Sounder (AIRS) instrument, among others. The AIRS instrument samples

the infrared spectral region with a much higher spectral resolution. AIRS covers the 3.7-µm to 15.4-µm region with a spectral resolution ($\lambda/\Delta\lambda$) of 1200, recording in 2378 infrared (IR) channels, and provides the capability to retrieve daily CO_2 concentration for the first time globally, over land, ocean and polar regions, day time and night time, even in the presence of clouds, with an accuracy better than 2ppmv (i.e., < 0.5%) (Aumann et al., 2005; Chaline et al., 2005). AIRS retrievals of CO total columns (TC) or CO profiles are the products of convolution of the true CO profile with a priori profile and averaging kernel (McMillan et al., 2009). AIRS retrievals for ascending orbits (around noon of local time) are reported separately from descending orbit (around midnight of local time). Carbon monoxide in the troposphere is routinely retrieved from thermal infrared measurements by Troposphere Emission Spectrometer (TES) on the NASA Aura Satellite launched in July 2004.

With the availability of FRP, attempts have been made to relate FRP with the amount of biomass consumed and/or the amount of smoke aerosols emitted. There is a linear relationship between the total FRE (i.e. time-integrated FRP) released over the lifetime of a fire and the total amount of fuel biomass consumed (Wooster et al., 2002, 2005). In addition to that, Ichoku and Kaufman derived another simple linear relationship between FRP and the rate of release of smoke particulate matter for different regions of the world. The latter, which was based on MODIS measurements, was confirmed in the laboratory using similar measurements of small scale fires (Ichoku et al., 2008b). Consequently, this has enabled the derivation of smoke emission coefficients such that whenever FRP is measured, the corresponding PM emission rate is instantly evaluated. As a result, satellite measured FRP could be used to realistically estimate the smoke emissions as well as the amount of biomass burned both from regional and global scale open-air biomass burning activities (Ichoku et al., 2008a).

Regional scale emission estimates for savanna fires are generally undertaken through model-based approaches that combine information on the amount of emitted gas species per unit mass of fuel burned, with estimates of the burned area, fuel load and the proportion of the available fuel actually combusted (Seiler & Crutzen 1980; Kasischke & Bruhwiler 2003). Importantly, the relative emission of different chemical compounds by fire is strongly dependent on the relative incidence of flaming and smoldering combustion. For instance, it is well known that, between 20% to 90% of total pyrogenic emissions of partially combusted products, such as smoke particulates, methane and CO are released during the smoldering stage (Scholes et al., 1996b; Hardy et al., 2001). AIRS is also an important new source of information about weather and climate processes. It was studied using correlative observations to show that AIRS total water vapor estimates have no cloud dependent biases. AIRS has provided over 300,000 globally distributed retrievals per day since September 2002, and has a five-year planned lifetime. Each retrieval includes profiles of temperature and water vapor (Fetzer et al., 2005).

Since FRE is related to Biomass burning, which in turn is related to emissions, it follows that FRE is itself related to emissions of particle matter and other species. In this research 4 regions were selected, they are Alaska, Brazil, Congo basin and West Africa. The FRP flux was extracted from MODIS measurements and interrelated with the CO_2 data, CO data, Surface air temperature and Water vapor data sets extracted from AIRS measurements. The FRP flux was

also interrelated with the Aerosol data sets form MODIS measurements. This comparison was done in a period of 7 year i.e. from 2003-2010.

METHODOLOGY

Data Sources

The data sets used for this study were obtained from two sources and stored in the American Standard Code for Information Interchange (ASCII) format. The data sets were obtained from the GIOVANNI website (http://disc.sci.gsfc.nasa.gov/giovanni/). GIOVANNI is a web-based application developed by the GES-DISC, which provides a simple and intuitive way to visualize, analyze, and access vast amounts of Earth Science remote sensing data without having to download the data. GIOVANNI is an acronym for the GES-DISC (Goddard Earth Sciences Data and Information Service Center) Interactive Online Visualization And aNalysis Infrastructure. All the data sets were extracted from Aqua Satellite measurements except TES-CO which was extracted from Aura Satellite. Only the daytime Aqua satellite data were used, because fire activity is dominant during the day- time. The calculation of area on each region was done using software known as Map tool 2.
Table 1: Showcases the coordinates of selected regions and area of the regions in square kilometers.

CO Data

The CO retrieval data were obtained from the AIRS Online Visualization and Analysis system. The data were analyzed by 1.0° x 1.0° grids of monthly, level-3 Product Version 5 (V5) standard products, and the parameter used was the total column CO_ ascending. The TES level-3 Daily Global surveys, Troposphere Emission Spectrometer Global 2.0° x 4.0° Gridded data was also used in analyzing the TES-CO data, and the parameter used was the CO total column density (Nadir).The visualization approach used was time series, from 2003-2010. The level 3 data products are geophysical parameters that have been spatially and temporally resample from levels 1 or 2 data.

CO_2 Data

AIRS Online Visualization and Analysis was used for the extraction of CO_2 data, from the 2.5° x 2.0° gridded monthly level 3 V5 standard products. The extracted parameter was CO_2_ Fraction (mole fraction). Time-series visualization was used to analyze data covering the period 2003-2010.

Aerosol Data

The MODIS instrument onboard the EOS Aqua satellite, has been acquiring moderate-resolution, spectral measurements of aerosol properties over both land and ocean, with near daily global average, since late February 2000 (King et al., 1999). Aerosol data were extracted from MODIS Aqua monthly Level 3 Version 5.1 data product, gridded at 1° x 1° spatial resolution;

Parameter extracted was Aerosol Optical Depth at 550nm. Visualization was by Time-series analysis of data for the period 2003- 2010.

FRP DATA

The MODIS sensor on the experimental polar orbiting Terra and Aqua satellites is the first sensor to enable retrievals of the Fire Radiative Power at a global scale [Justice et al., 2002]. FRP is the spatially integrated instantaneous radiative energy emitted by all fires within the satellite pixel (Wooster et al., 2003).

$$FRP = A_{sa}\, \varepsilon\sigma \sum f_i \;\; T^4{}_i$$

Where A = the total area of the satellite pixel [m^2]
ε = fire emissivity
σ = Stephan-Boltzmann constant [$5.67 \times 10^{-8}\ J^{-1}m^{-2}K^{-4}$]
f_i = fractional area of the ith thermal component
T_i = temperature of the ith thermal component [K].

The FRP data of the fire pixels within the boundaries of each of the regions of interest were extracted. Using the visible reflectance data from the MODIS fire dataset ("R2"), as proxy for day/night flags (daytime represented by positive reflectance, and nighttime otherwise) the daytime FRP data were extracted and used.

Total Water Vapor and Surface Air Temperature Data

AIRS Online Visualization and Analysis was used to extract the gridded 1.0° x 1.0° monthly level 3 version 5 standard products. Surface air temperature_ ascending and total column water vapor _ ascending were the parameters selected because we wanted the data set acquired during the daytime. Visualization was done using Time series of data covering the period 2003 – 2010.

RESULTS AND DISCUSSION

Figure 1, shows the SCIAMACHY image of Carbon dioxide from 2003 – 2005, and the Carbon dioxide increase in the troposphere in ppm (part per million). The result retrieved from the 4 regions show similar patterns in figure 2. The main increase in CO_2 in these regions may be attributed to anthropogenic activities such as forest fire, biomass burning, industrial emission etc, or the transportation of CO_2 by wind. This is, because the level of CO_2 increase in each of these regions was between 0.016 g – 0.0176g from 2001 – 2008.

Effects of FRP on the emission of CO

Wildfire or biomass burning is not the only contributor of CO in the troposphere. However, from the figure 3, it shows that an increase in FRP causes an increase in CO emission during the fire season of the year in each region. In figure 3c, the FRP data obtained for Alaska indicates very low forest fire from 2001- 2010, compared with other regions that were selected. The summer peak fires occur only in Alaska. The peak fire season for Congo basin is fall, while that of West Africa and Brazil is in winter. Indicating the period in which most of the biomass burning, and forest fire occurred in Alaska, Brazil Amazon, West Africa and Congo Basin. The CO emission in Alaska shows that biomass burning contributes less amount of CO in the troposphere. The CO present may be due to transportation from other regions or other anthropogenic activities. Congo Basin has two seasons the rainy season (spring) and the dry season (summer). In figure 3d emission of CO in the spring is low compared to the summer, and FRP is also low in the spring. In figure 3c between 2008 -2010 the FRP graph was decreasing due to the government laws protecting the deforestation of the Brazil Amazon.

Effects of FRP on the emission of Aerosol

Aerosol is a suspension of fine solid particles such as smoke, smog etc. Aerosols can be emitted from various sources like volcanoes, dust storms, forest and grassland fires, burning of fossil fuels in vehicles, power plants etc. In figure 3c, Alaska shows little similarity between the peaks in the FRP and the aerosol data sets. Aerosol emission occurs in different seasons of the year. Congo Basin and West Africa shows aerosols are detected by the MODIS sensor immediately after the dry season (summer) while that for Brazil Amazon was detected during the summer of each year. In figure 3b from 2008- 2010 the emission of aerosol is low compared to the other years. This also indicates that wildfire contributes majority of the aerosols into the troposphere in the Brazil Amazon.

How FRP interrelates to the Surface Air Temperature

Surface air temperature is the temperature of the air near the surface of the earth. In figure 4 the surface air temperature is relatively high, when the FRP data sets are at their highest peak in each region. In figure 4a (West Africa) the surface air temperatures continue to increase after the dry season (summer). This result indicates that biomass burning probably contributes to the change in surface air temperature in each of the regions.

How FRP interrelates to the Total Water Vapor

Water vapor or aqueous vapor is the gas phase of water. Water vapor is one state of water within the hydrosphere; water vapor can be produced from evaporation or from the sublimation of ice. In figure 4 it is shown clearly in Brazil Amazon, West Africa and Congo Basin that the water vapor's highest peak occurs during the spring season and lowest peak during the summer. This shows that there is probably no relationship between fires and atmospheric water vapor in these

regions. In contrast, figure 4c, shows a compelling graph for Alaska, which indicates that FRP increases as the water vapor increases. This is probably because the biomass burning in this region are mainly wildfire, and may be affecting mostly non-dry vegetation and releasing its water content in the form of water vapor.

Comparison between TES-CO and AIRS-CO

TES has higher spatial and spectral resolution compared to AIRS. However, TES global coverage is significantly less, with nadir pixels being only 5 x 8 km^2 in comparison to AIRS's retrieval grid of 45 x 45 km^2, and a swath width of 1600km across track (Warner et al., 2010). Therefore, because of the limited global coverage of TES data set and other reasons, TES-CO data looks unreliable compared to AIRS data in figure 5.

CONCLUSION

This research has been done to compare some of the principal emitted species in biomass burning smoke over four regions of the world located in Alaska, Brazil, the Congo basin, and West Africa. This study shows that biomass burning occurs in a specific season of the year in each region, producing aerosol, CO and CO_2 emissions in the process. The CO_2 in each region increases continuously beyond the biomass-burning season as the years go by. This is because CO_2 emission cannot be attributed to biomass burning alone, and accumulates over time because of its relatively long atmospheric lifetime. It also shows that biomass burning has an effect on the surface air temperature and water vapor at least in these regions.

Acknowledgements

This work was done as a requirement for fulfilling my internship responsibilities at NASA Goddard. Although it was only for a short time, it helped me in many different ways in knowing more about the earth, climate change and also in strengthening my career in Atmospheric Chemistry. This would not have happened without the kind and appropriate guidance of my mentor, Dr Charles Ichoku and also Luke Ellison for his assistance. I would also like to thank Valerie Casasanto, Dr Ali Tokay and Dr Jeffrey B. Halverson for coordinating this program. I am very grateful for the opportunity to work at NASA Goddard and to all my friends at GSSP and other program.

REFRENCES

Aumann, H.H., D. Gregorich, and S. Gaiser (2005), AIRS hyper-spectral measurements for climate research: Carbon dioxide and nitrous oxide effects, *Geophys. Res. Lett.*, *32*, L12802, doi: 10.1029/2005GL022564.

Boering, K. A, S. C. Wofsy, B. C. Daube, H. R. Schueider, M. Loewenstein, J. R. Podolske, and T. J. Conway (1996), Stratospheric mean ages and transport rates from observations of carbon dioxide and nitrous oxide, *Science*, *274*, 1340-1343.

Conway, T., P. P. Tans, L. S. Waterman, K. W. Thoning, D. Kitzis, K. Masarie, and N. Zhang (1994), Evidence for interannual variability of carbon cycle from the national oceanic and atmospheric administration climate monitoring and diagnostics laboratory global air sampling network*, J. Geophys. Res., 99*, 22831-22855.

Chahine, M., C. Barnet, E. T. Olsen, L. Cheu, and E. Maddy (2005), On the determination of atmospheric minor gases by the method of vanishing partial derivatives with application to CO_2, *Geophys. Res. Lett., 32,* L22803, doi: 10.1029/2005GL024165.

Fetzer, E., A. Eldering and L. Sung-Yung, Characterization of AIRS temperature and water vapor measurement capability using correlation observations. AMS 85th Annual Meeting, San Diego, CA, 2005.

Ichoku, C., and Y. J. Kaufman (2005), A method to derive smoke emission rates from MODIS fire radiative energy measurements, *IEEE transactions on geosciences and remote sensing, Vol 43*, No 11, pp. 2636-2649.

Ichoku, C., L. Giglio, M. J. Wooster, and L. A. Remer (2008a), Global characterization of biomass-burning patterns using satellite measurements of fire radiative energy. *Remote sensing of Environment*, *112*, pp. 2950-2962.

Ichoku, C., J. V. Martins, Y. J. Kaufman, M. J. Wooster, P. H. Freeborn, W. M. Hao, S. Baker, C. A. Ryan, and B. L. Nordgren (2008b), Laboratory investigation of fire radiative energy and smoke aerosol emissions, *Journal of Geophysical Research*, *113*, D14509, doi:10.1029/2007JD009659.

Indermühle, A., B. Stauffer, and T. F. Stocker (1999), Early Holocene atmospheric CO_2 concentrations, *Science*, *286*, 1815.

Intergovernmental Panel on Climate change (2001), *Climate change 2001*: *The Scientific Basis*, edited by J. T. Houghton et at., Cambridge Univ. Press, New York.

Justice, C. O., L. Giglio, S. Korontzi, J. Owens, J. Morisette, D. Roy, D. J. Descloitres, S. Alleaume, F. Petitcolin, and Y. Kaufman, The MODIS fire products, *Remote Sens. Environ*., Vol. 83, pp. 244-262, 2002.

Kasischeke ES, Bruhwiler LP (2003) Emissions of carbon dioxide, carbon monoxide, and methane from boreal forest fires in 1998. *Journal of Geophysical Research* **108**, 8146.

King, M. D., Y. J. Kaufman, D. Taure, and T Nakajima, Remote sensing of troposheric aerosols from space: Past, present and future, *Bull. Am. Meteorol. Soc., 80*, 2229-2259, 1999.

Keeling , C. D., S. C. Piper, and M. Heimann (1989), A three dimensional model of atmospheric CO_2 transport based on observed winds: 4, mean annual gradients and interannual variations, in *Aspects of Climate Variability in Pacific and the Western Americas*, *Geophys, Monogr. Ser.,* Vol. 55, edited by D. H. Peterson, pp. 305-363, AGU, Washington, D.C.

Kaufman, Y. J., Justice, C. O., Flynn, L. P., Kendall, J.D., Prius, E. M., Giglio, L. et al. (1998). Potential global fire monitoring from EOS-MODIS. *Journal of Geophysical Research, 103*, 32215-32238.

Logan, J. A., Prather, M. J., Wofsy, S. C., and McElroy, M. B.: Troposphere chemistry: A global perspective, *J. Geophys. Res., 86*, 7210-7254, 1981.

McMillan, W. W. Evans, K., Barnet, C., Maddy, E., Sachse, G., and Diskin, G.: AIRS Version 5 CO Retrieval: Algorithm Description and Validation, IEEE Transactions on Geoscience and Remote Sensing, in press, 2009.

Schüle, W., Landscapes and climate in prehistory: Interactions of wildlife, man and fire, in *Fire in the Tropical Biota: Ecosystem Processes and Global Challenges*, edited by J. Goldammer, pp. 273-318, Springer-Verlag, New York, 1990.

Seiler, W., Crutzen P. J., (1980) Estimates of gross and net fluxes of carbon between the biosphere and the atmosphere from biomass burning, *Clim. Change,2*, 207-247.

Scholes R. J., Ward D.E., Justice C. O., (1996b) Emission of trace gases and aerosol particles due to vegetation burning in southern hemisphere Africa. *Journal of Geophysical Research* **101**, 23677-23682.

Wooster M. J., B. Zhukoz and D. Oertel, Fire radiatve energy for quantitative study of biomass burning: derivation from the BIRD experimental satellite and comparison to MODIS fire product. *Remote Sens. Environ.* **86***,* pp. 83-107, 2003.

Wooster, M. J. (2002), Small-scale experimental testing of fire radiative energy for quantifying mass combusted in natural vegetation fires. *Geophysical Research Letters*, **29**, 2027.doi: 10.1029/2002GL015487.

Wooster, M. J., G. Roberts, G. L. W. Perry, and Y. J. Kaufman (2005), Retrieval of biomass combustion rates and totals from fire raditive power observations: FRP derivation and calibration relationships between biomass consumption and fire radiative energy release, *Journal of Geophysical Research*, *110*, D24311.doi:10.1029/2005JD006318.

Warner, J. X., Wei Z., Strow, L. L., Barnet, C. D., Sparling, L. C., Diskin G., and Sachse G.: Improved agreement of AIRS tropospheric carbon monoxide product with other EOS sensors using optimal estimation retrievals: *Atmos. Chem. Phys. Discuss., 10*, 11851-11884, 2010.

TABLE

Table 1: showcases the coordinates of selected regions and Area of the regions in square kilometers.

Region	Latitude Range		Longitude Range		Area of Land (Km^2)
	Min Lat	Max Lat	Min Lon	Max Lon	
ALASKA	61.5	69.2	-156.4	-142.3	5.58×10^5
CONGO BASIN	-3.9	8.7	10.9	28.0	2.68×10^6
BRAZIL AMAZON	-13.2	-0.6	-63.3	-47.8	2.40×10^6
WEST AFRICA	6.4	13.1	-10.2	12.0	1.85×10^6

Figures 1

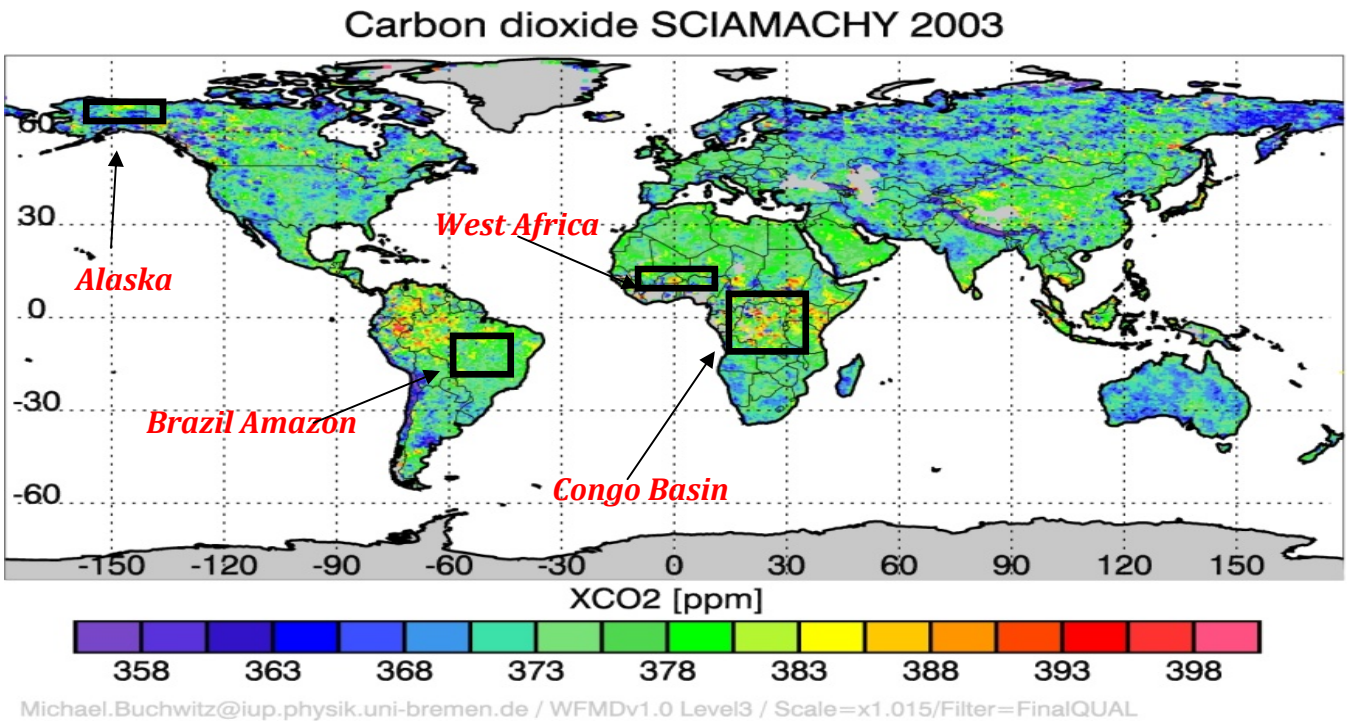
Carbon dioxide SCIAMACHY 2003
West Africa
Alaska
Brazil Amazon
Congo Basin
60
30
0
-30
-60
-150 -120 -90 -60 -30 0 30 60 90 120 150
XCO2 [ppm]
358 363 368 373 378 383 388 393 398
Michael.Buchwitz@iup.physik.uni-bremen.de / WFMDv1.0 Level3 / Scale=x1.015/Filter=FinalQUAL

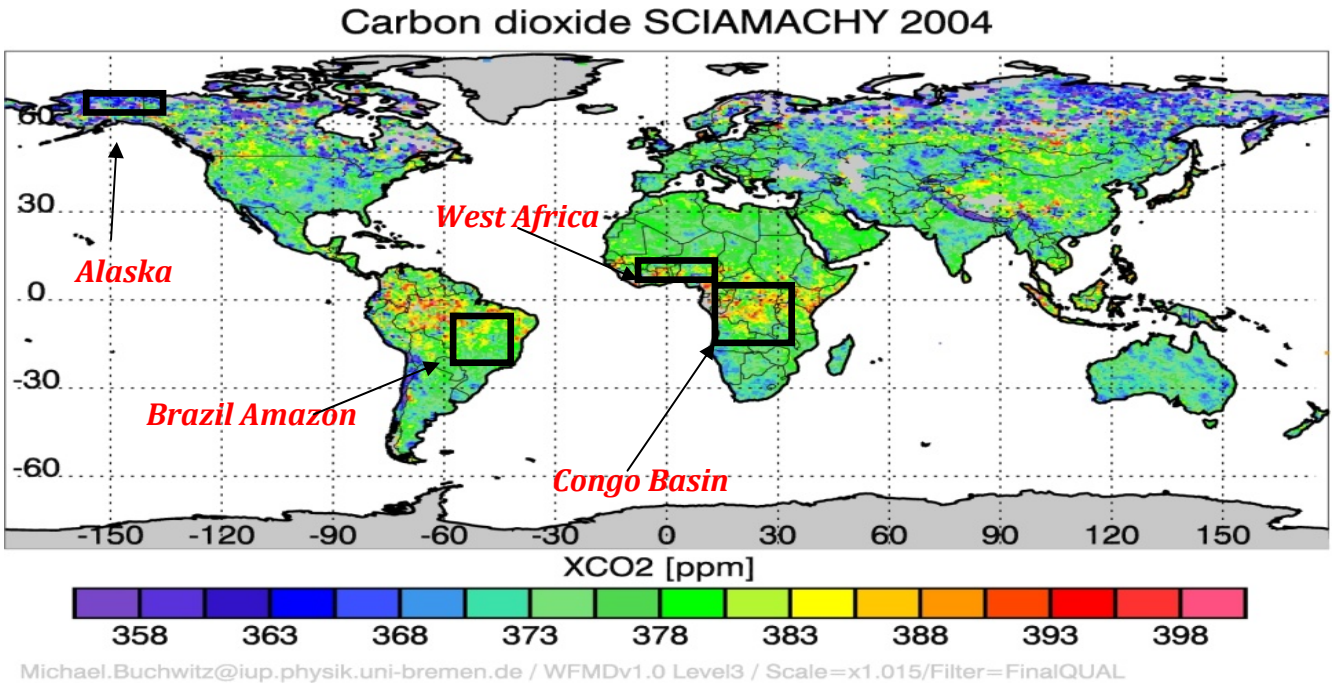
Carbon dioxide SCIAMACHY 2004
West Africa
Alaska
Brazil Amazon
Congo Basin
60
30
0
-30
-60
-150 -120 -90 -60 -30 0 30 60 90 120 150
XCO2 [ppm]
358 363 368 373 378 383 388 393 398
Michael.Buchwitz@iup.physik.uni-bremen.de / WFMDv1.0 Level3 / Scale=x1.015/Filter=FinalQUAL

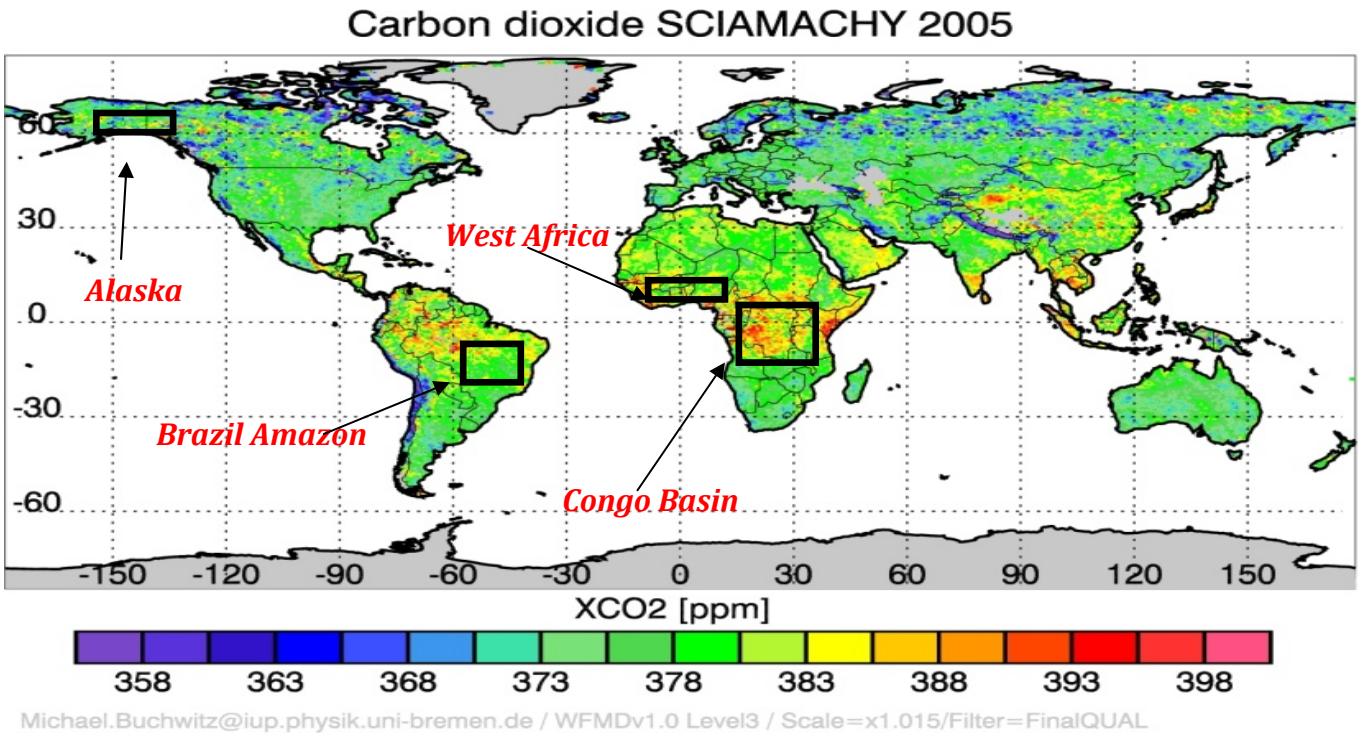

Figure 2

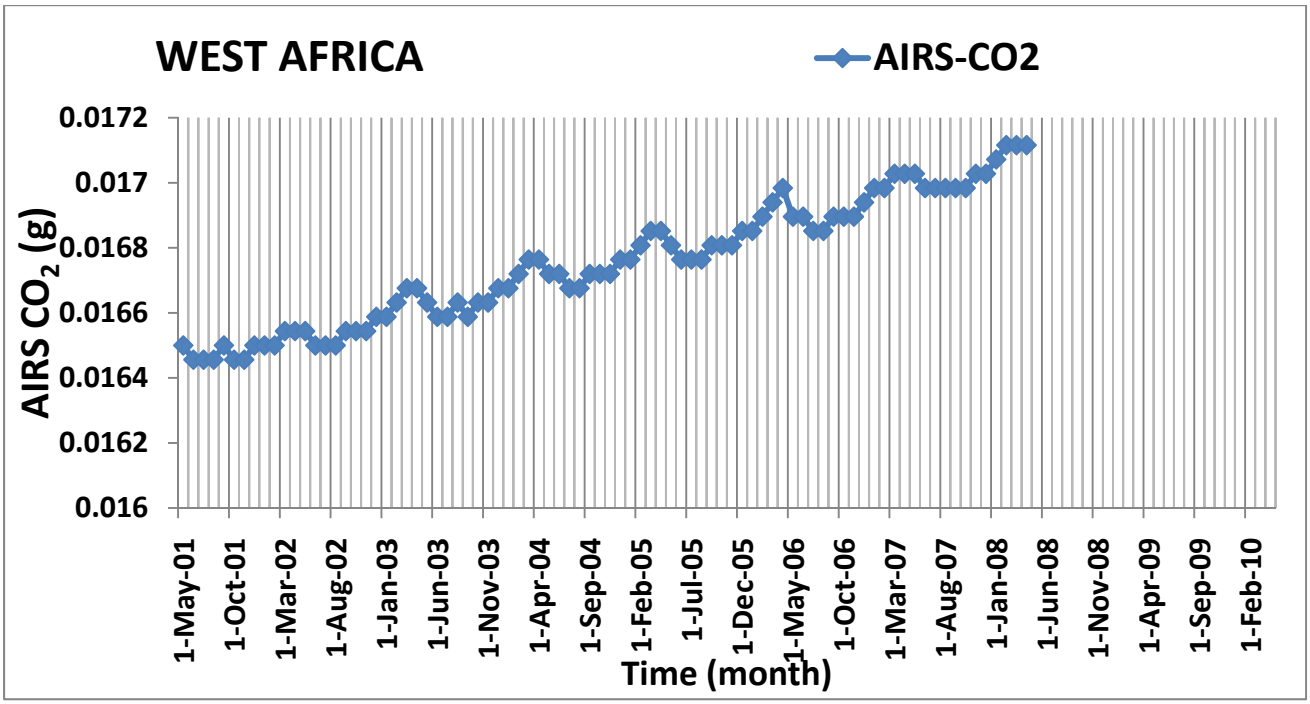

Fig. 2a shows the increase of Carbon dioxide in West Africa from 2001 – 2008.

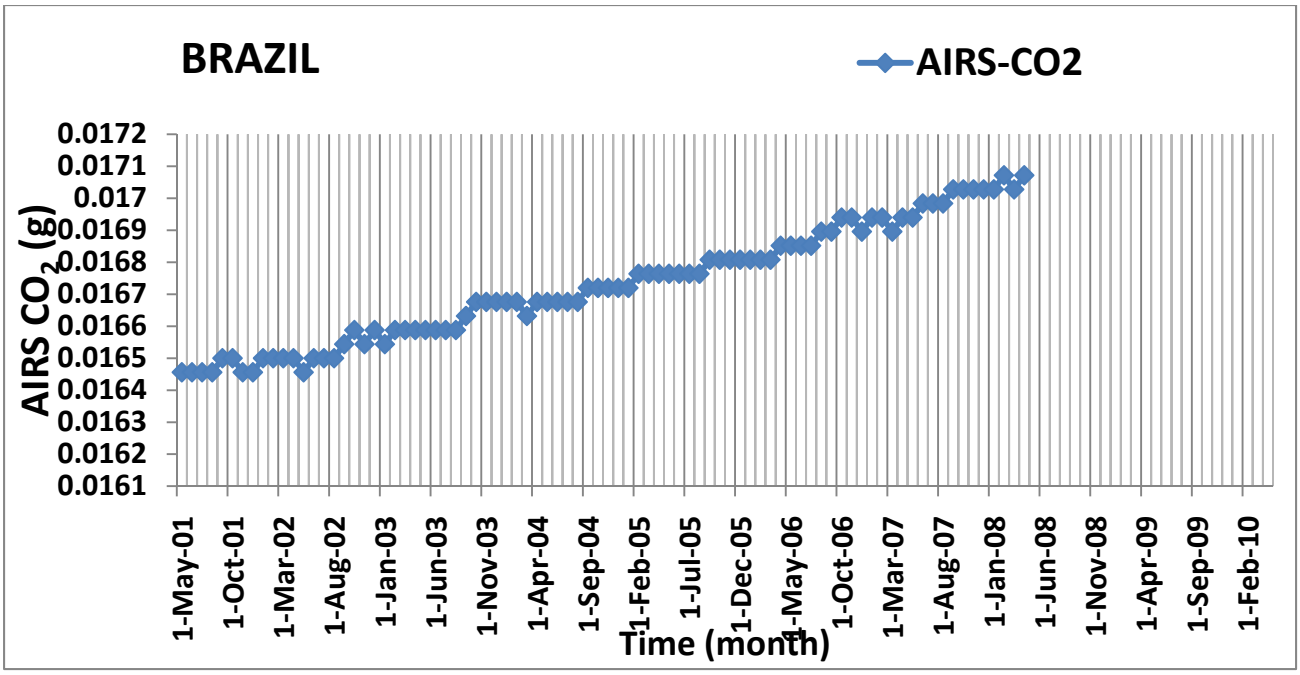

Fig. 2b shows the increase of Carbon dioxide in Brazil Amazon from 2001 – 2008.

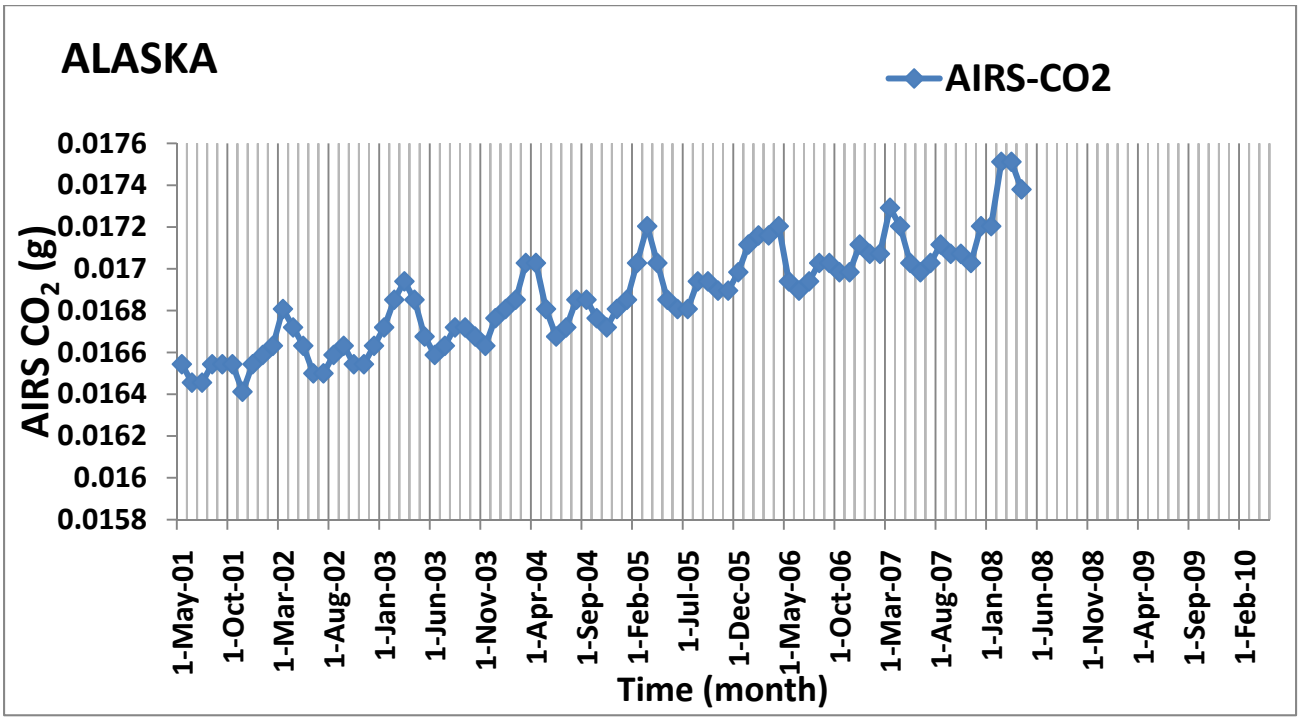

Fig. 2c shows the increase of Carbon dioxide in Alaska from 2001 – 2008.

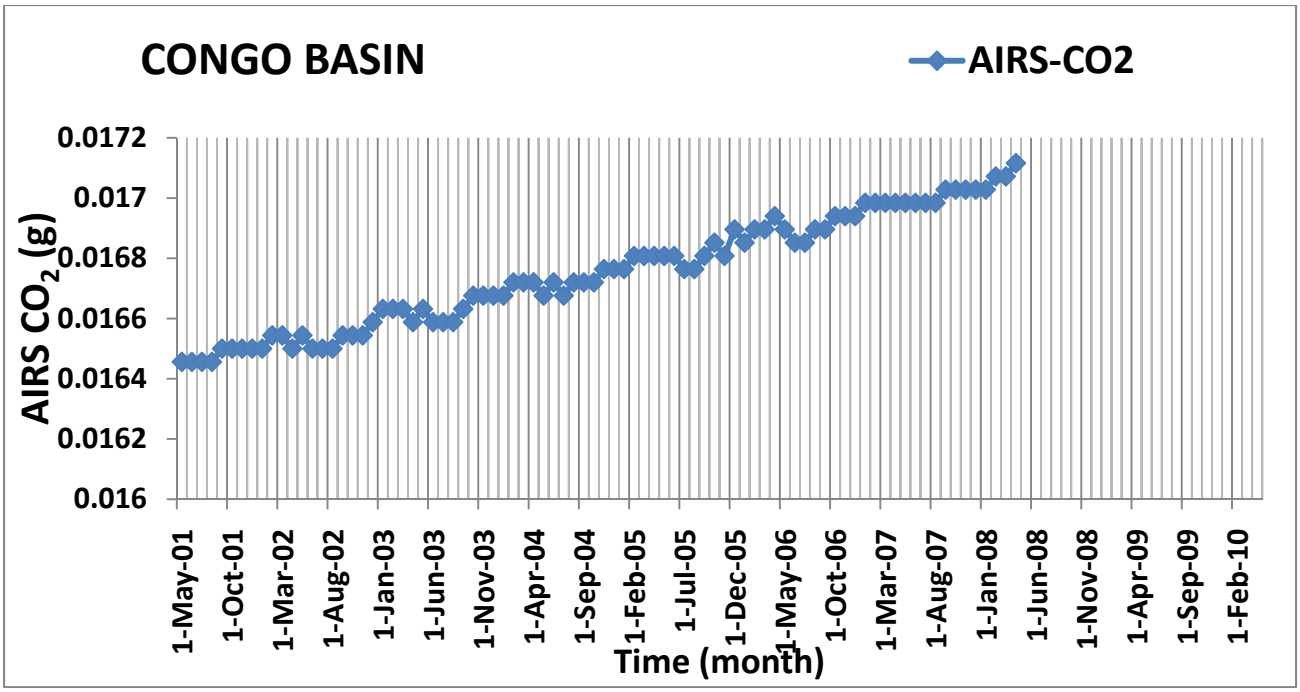

Fig. 2d shows the increase of Carbon dioxide in Congo basin from 2001 – 2008.

Figure 3

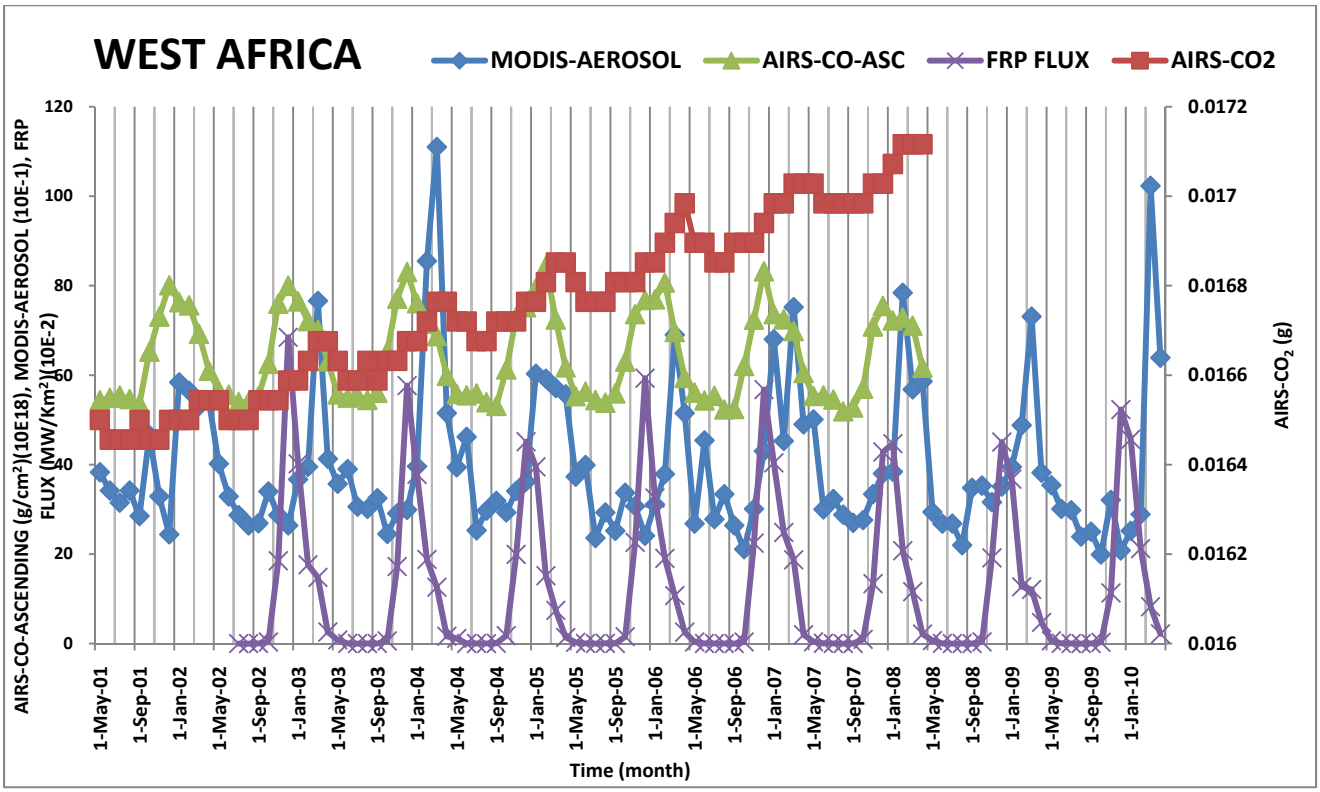

Fig. 3a shows the interrelationship between the Fire Radiative Power (FRP) and AIR-CO, AIR-CO_2, MODIS-AEROSOL in West Africa from 2001-2010.

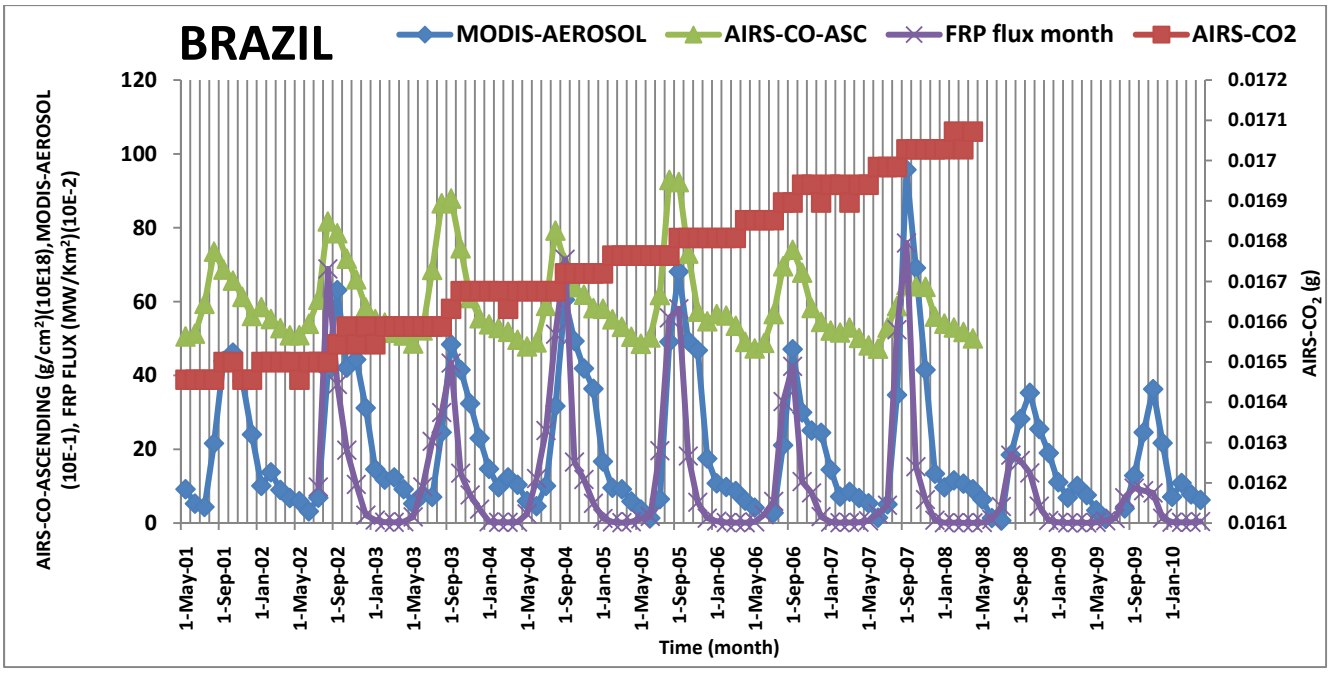

Fig 3b shows the interrelationship between the Fire Radiative Power (FRP) and AIR-CO, AIR-CO_2, MODIS-AEROSOL in Brazil from 2001- 2010.

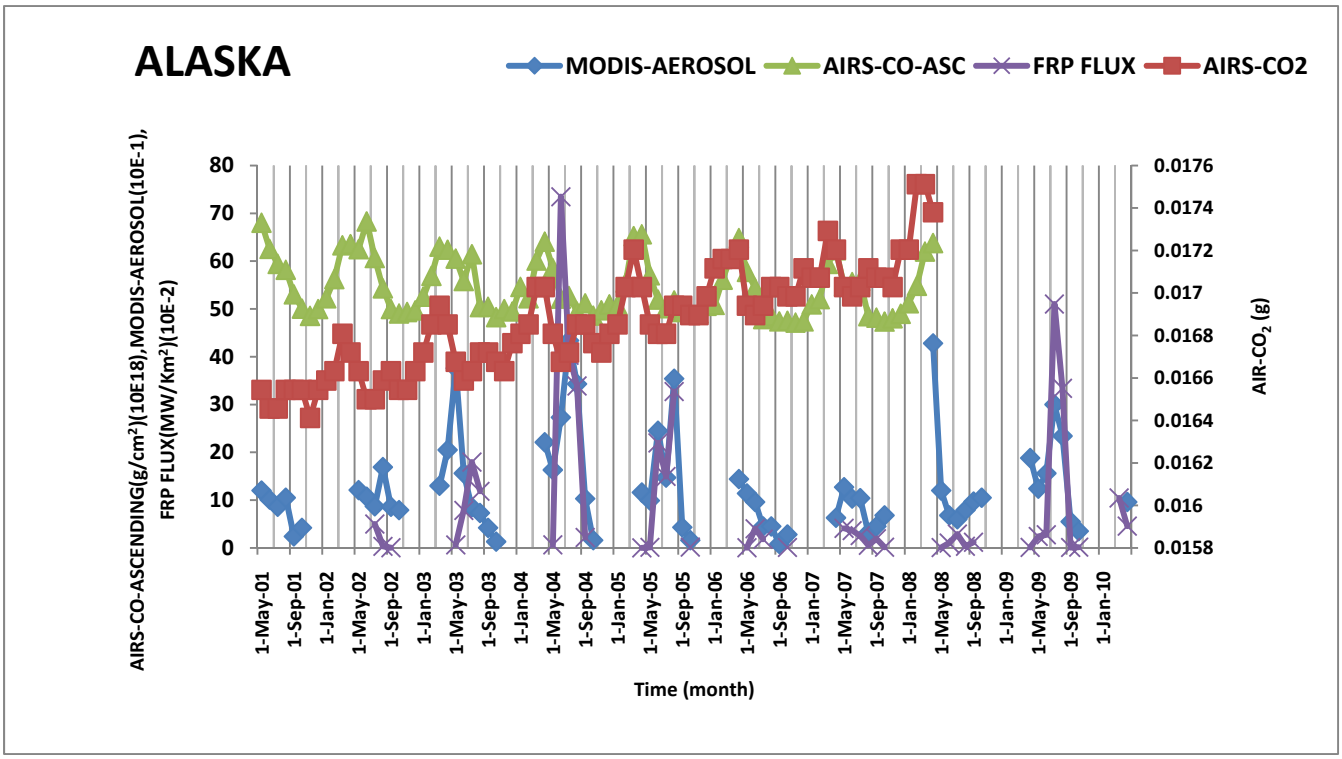

Fig 3c shows the interrelationship between the Fire Radiative Power (FRP) and AIR-CO, AIRS-CO_2, MODIS-AEROSOL in Alaska from 2001-2010.

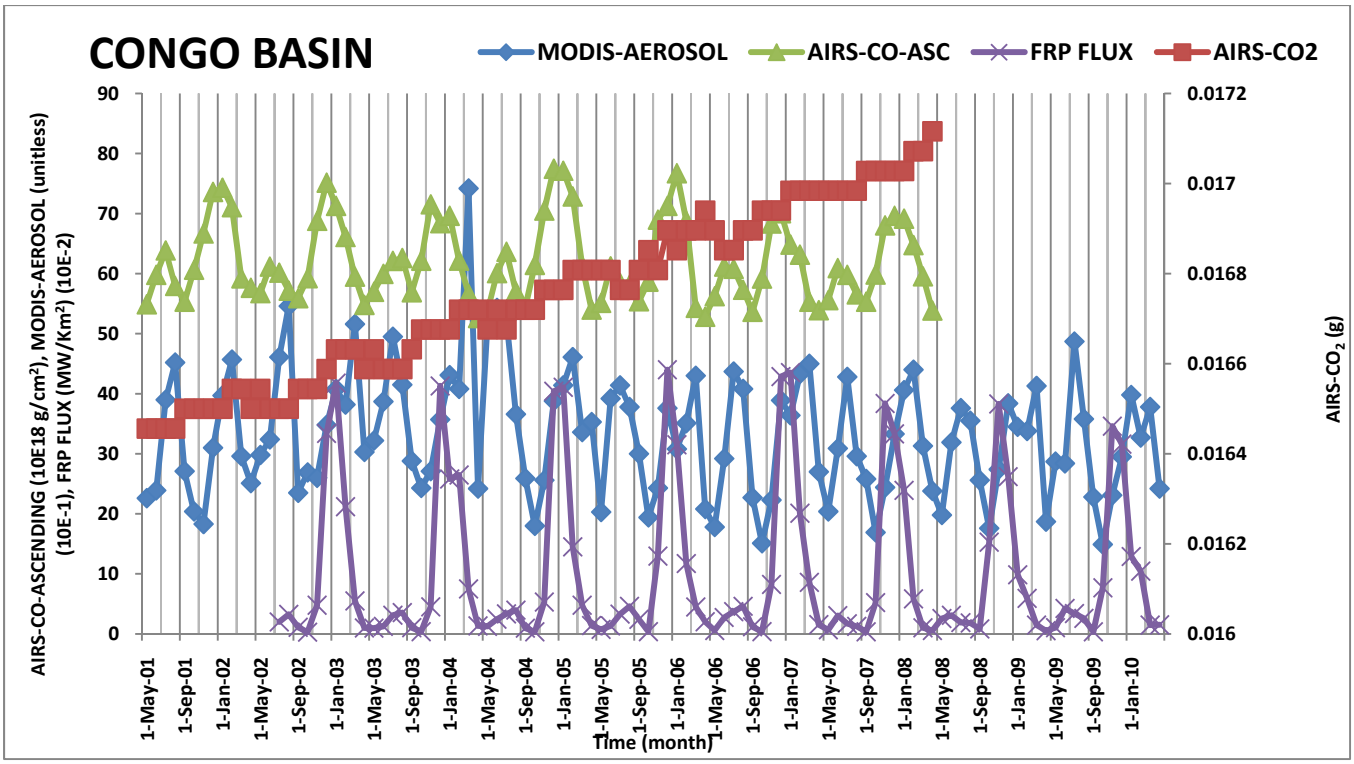

Fig 3d shows the interrelationship between the Fire Radiative Power (FRP) and AIR-CO, AIR-CO_2, MODIS-AEROSOL in Congo Basin from 2001- 2010.

Figure 4

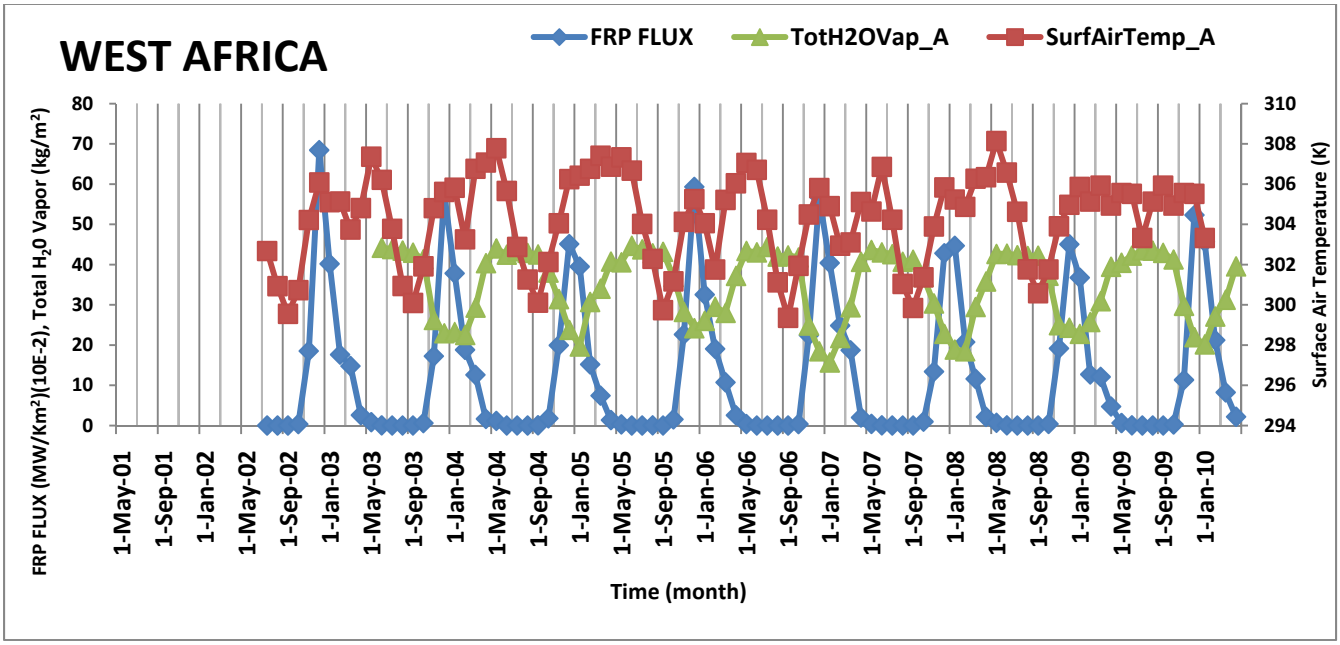

Fig.4a shows the graph of FRP, Surface Air Temperature and Total H_2O Vapor in West Africa from 2002 – 2010.

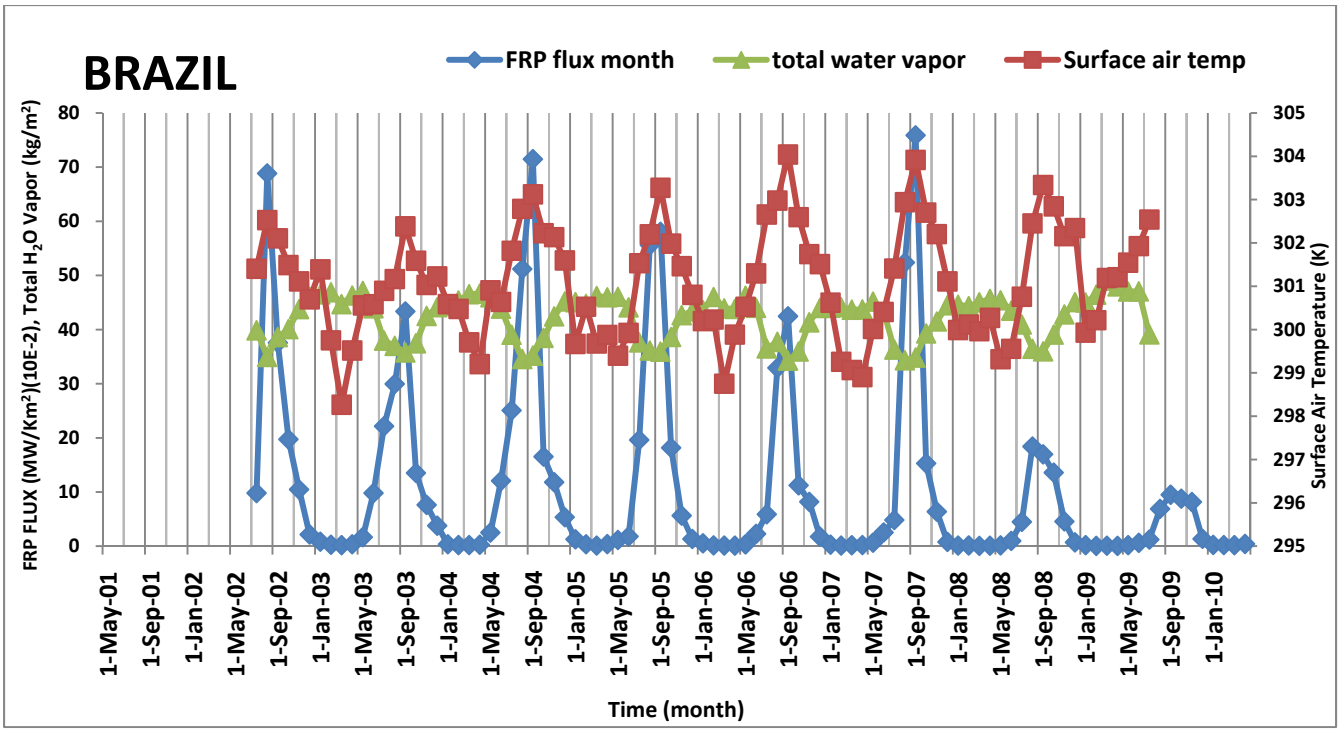

Fig.4b shows the graph of FRP, Surface Air Temperature and Total H_2O Vapor in Brazil Amazon from 2002 – 2010.

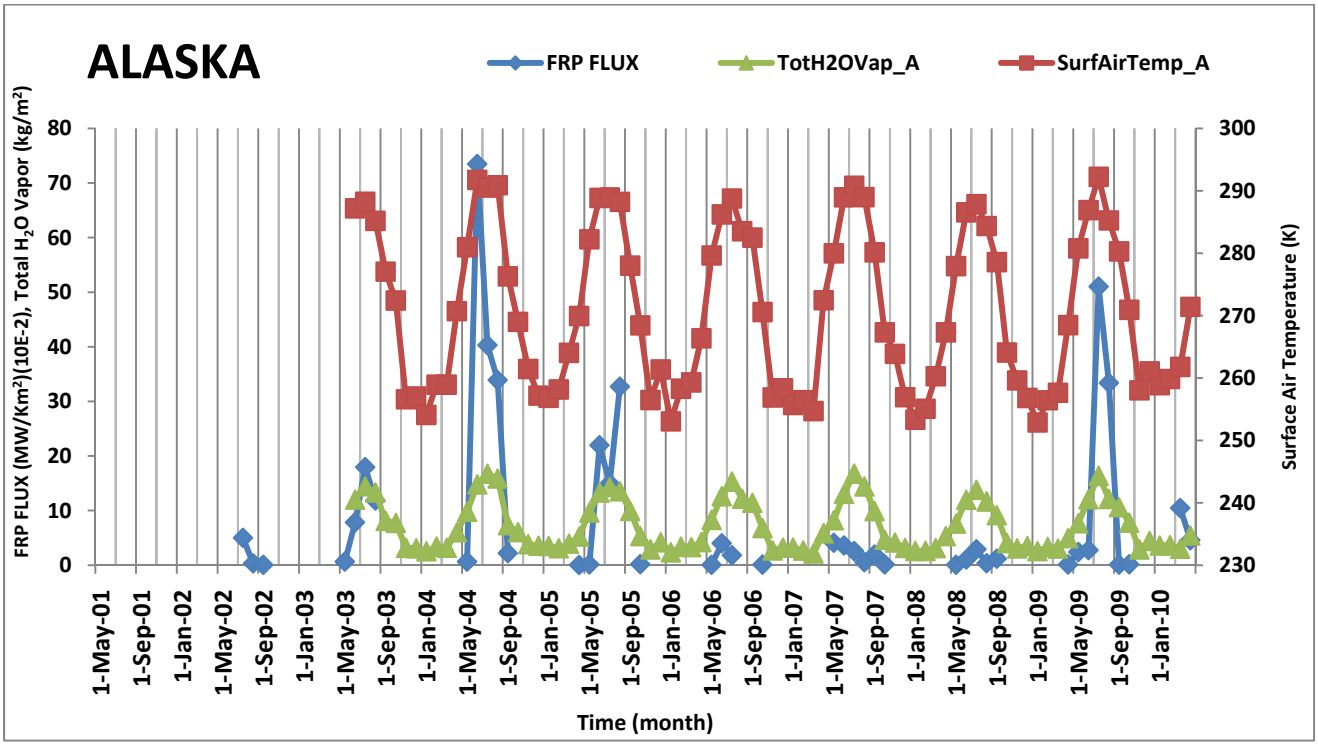

Fig.4c shows the graph of FRP, Surface Air Temperature and Total H_2O Vapor in Alaska from 2002 – 2010.

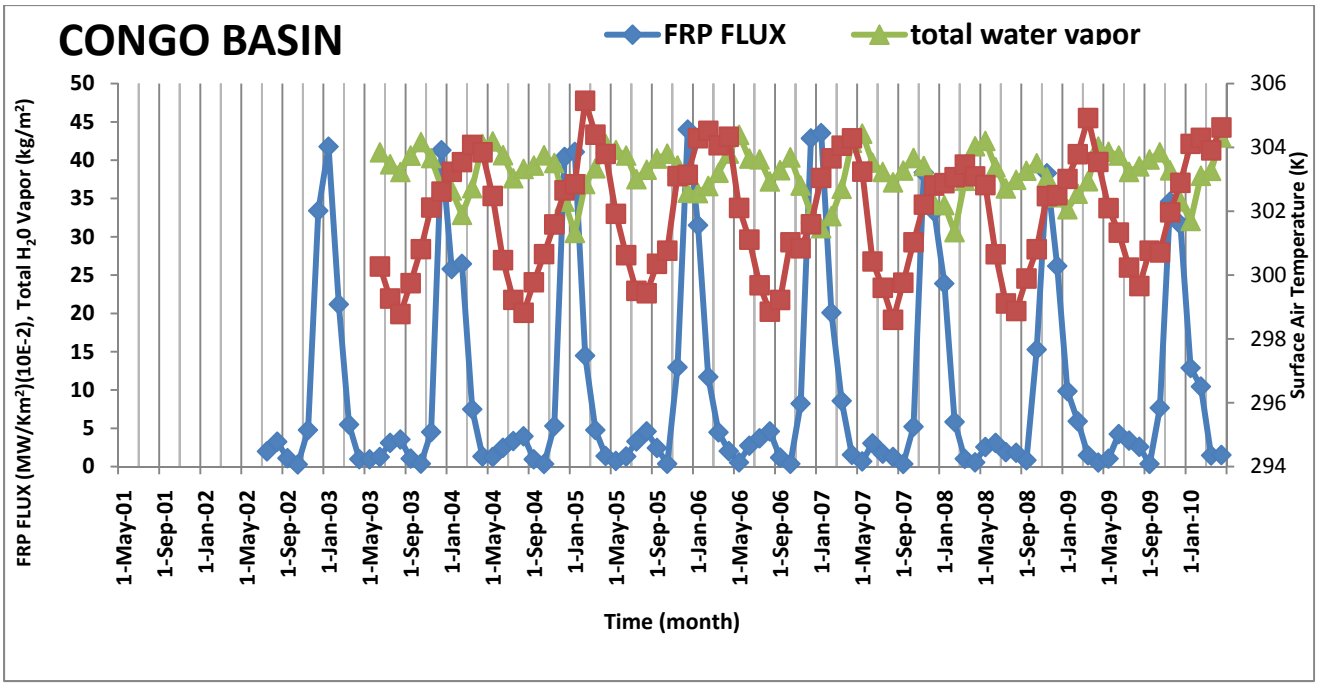

Fig.4d shows the graph of FRP, Surface Air Temperature and Total H_2O Vapor in Congo Basin from 2002 – 2010.

Figure 5

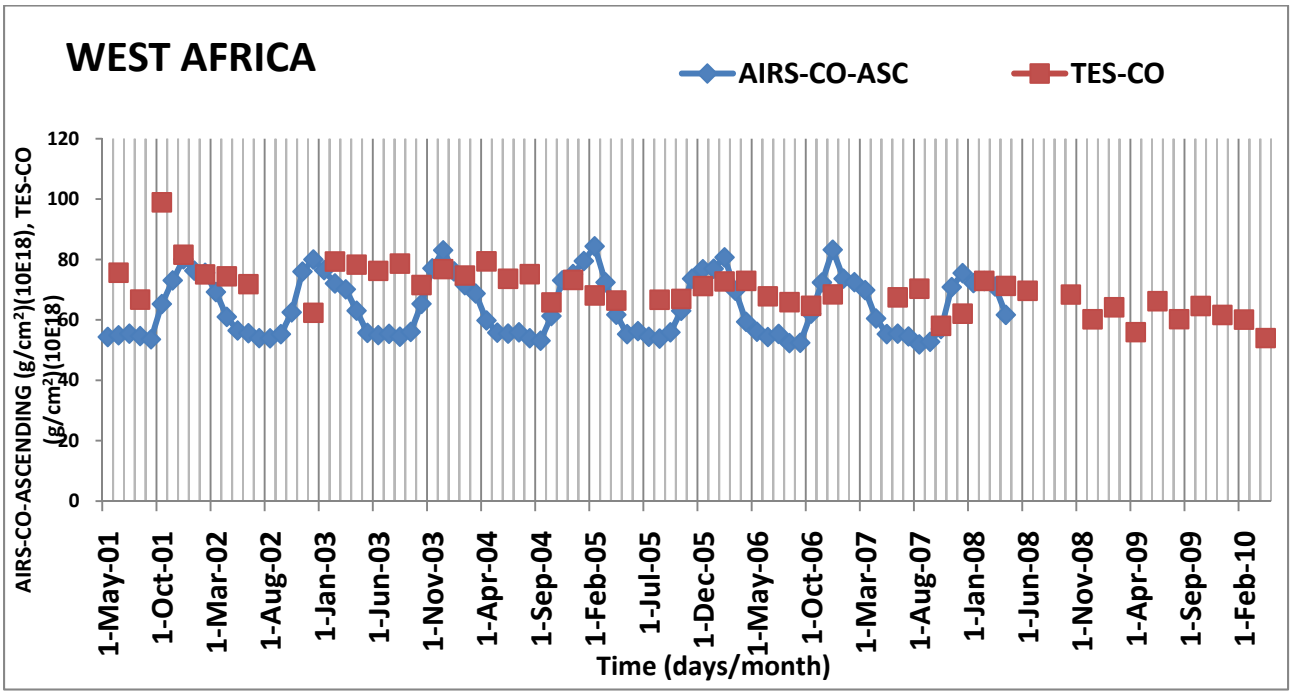

Fig 5a shows the comparison of data sets from TES-CO and AIRS-CO in West Africa from 2001-2010.

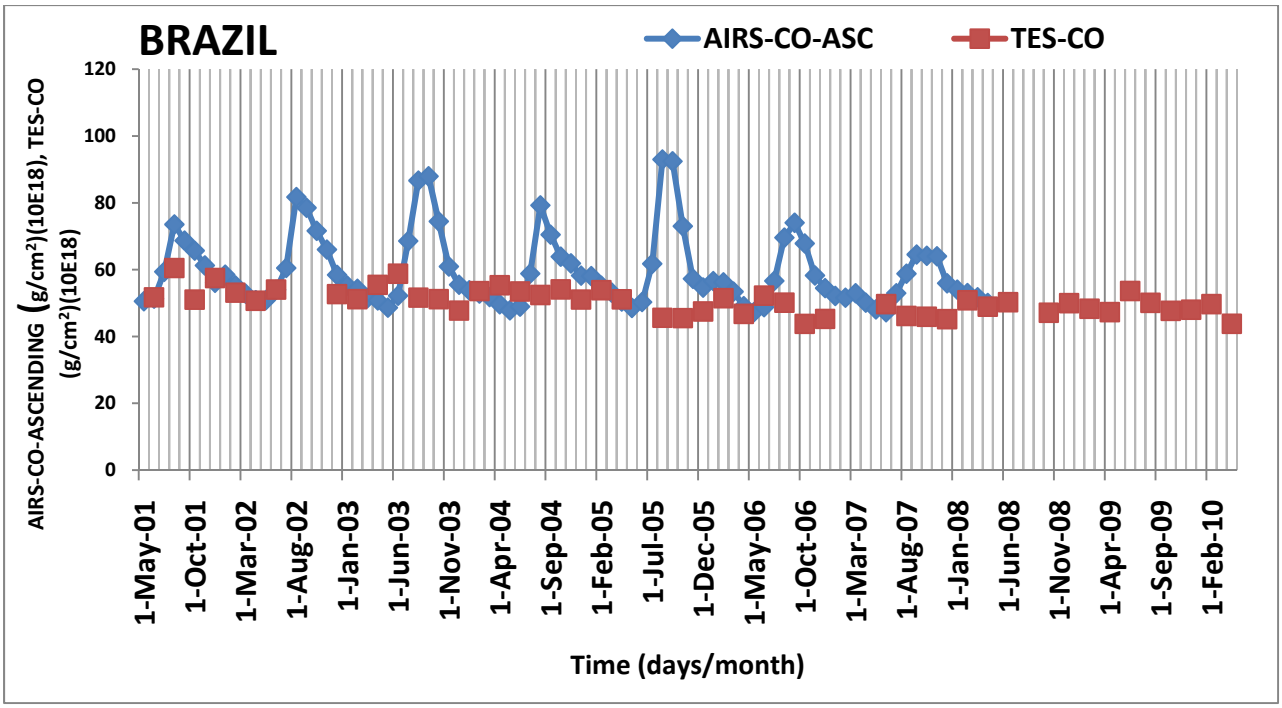

Fig 5b shows the comparison of data sets from TES-CO and AIRS-CO in Brazil from 2001-2010.

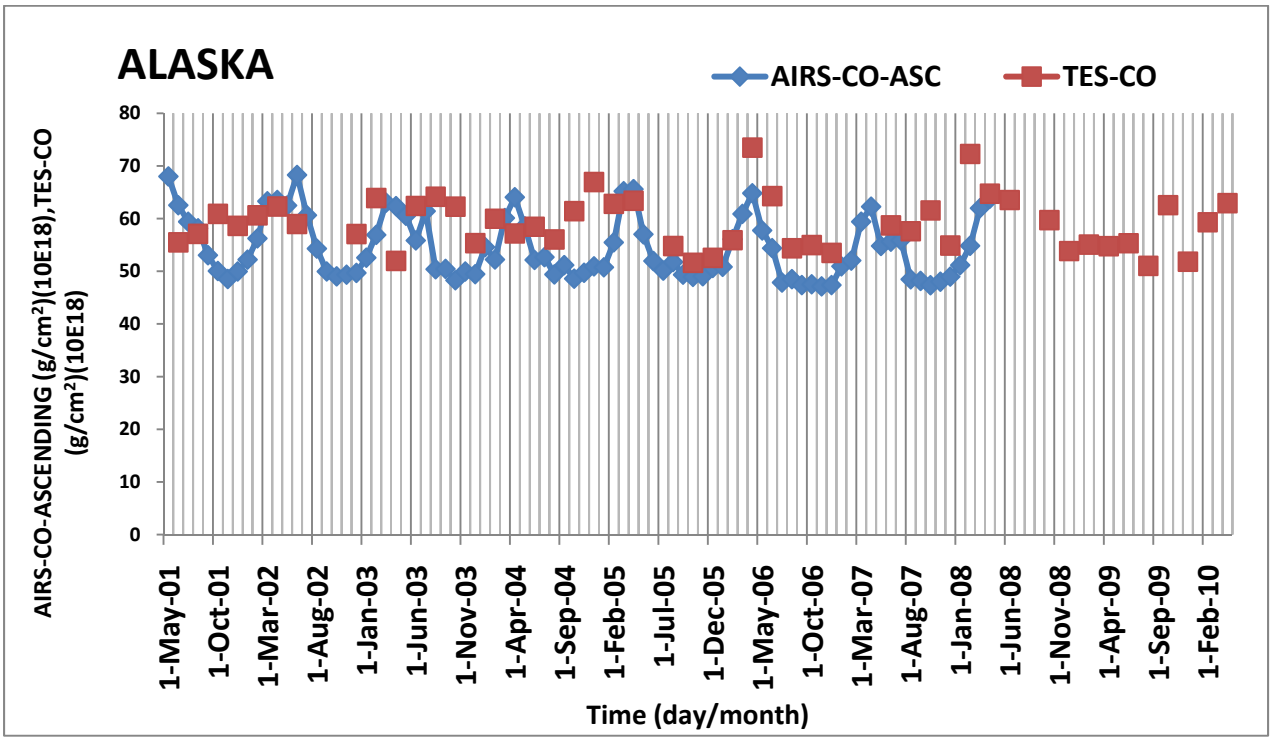

Fig 5c shows the comparison of data sets from TES-CO and AIRS-CO in Alaska from 2001-2010.

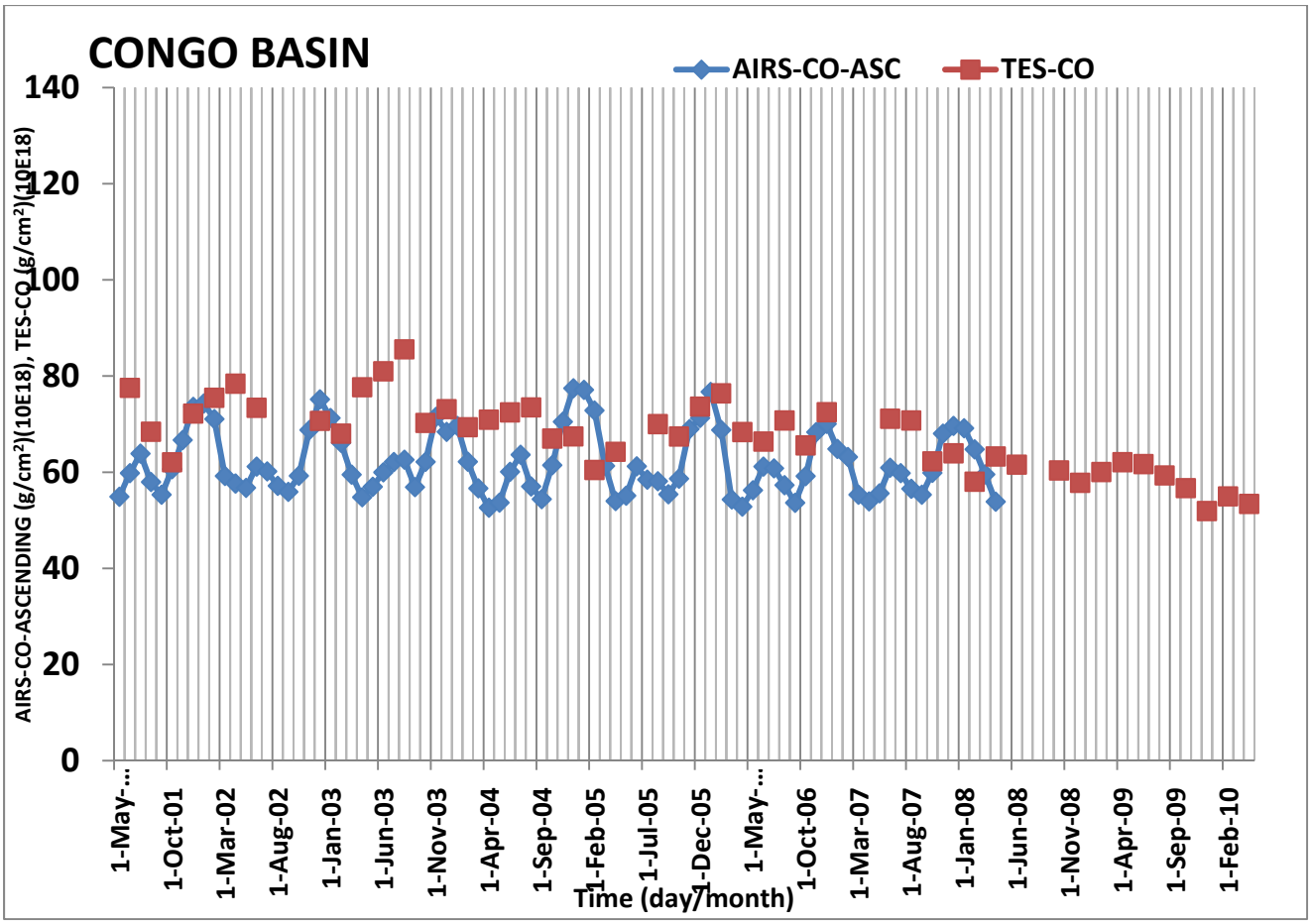

Fig 5d shows the comparison of data sets from TES-CO and AIRS-CO in Congo Basin from 2001-2010.